STUDIA UBB CHEMIA, LXIV, 2,Tom I, 2019 (p. 139-157)
(RECOMMENDED CITATION)
DOI:10.24193/subbchem.2019.2.12

Dedicated to Professor Florin Dan Irimie on the Occasion of His 65th Anniversary

MATHEMATICAL MODELLING AND PREDICTION OF CONGO RED ADSORPTION ON CHERRY STONES ACTIVATED CARBON

ANDREI SIMION[a], CRISTINA GRIGORAȘ[a*], LIDIA FAVIER[b], LUCIAN GAVRILĂ[a*]

ABSTRACT. The present paper was aimed to establish mathematical models useful to reduce the time required to discover the appropriate adsorption conditions of Congo Red (an intensively used organic dye) on an activated carbon prepared from cherry stones through calcination. To this purpose, various values of three parameters known as influencing the process, namely dye initial concentration (200 mg/L to 1000 mg/L), *p*H (2 to 12) and contact time (10 to 180 minutes) between the adsorbent and the adsorbate were variated. The recorded results of the adsorption process were used as data for Response Surface Methodology and Artificial Neural Network and several mathematical equations were generated. The conducted statistical analyses revealed that these equations can accurately express the Congo Red elimination from aqueous solutions. Moreover, the developed procedure is able to predict the process evolution in different conditions than those experimentally tested.

Keywords: *Adsorption, Artificial Neural Network, cherry stone, Congo Red, mathematical modelling, Response Surface Methodology, water treatment*

INTRODUCTION

Colored wastewater coming from various industries is considered a major source of environmental concerns. Besides being responsible for the unwanted visual effect, due to their chemical structures, dyes are often characterized by a reduced biodegradability being difficult to remove by classical wastewater treatments [1]. Moreover, most of the dyes can also negatively affect

[a] *"Vasile Alecsandri" University of Bacău; Faculty of Engineering; Department of Food and Chemical Engineering; Calea Mărășești 157, RO-600115, Bacău, România*
[b] *Univ. Rennes, Ecole Nationale Supérieure de Chimie de Rennes; CNRS, UMR 6226; 11 Allée de Beaulieu, CS 50837, 35708 Rennes Cedex 7, France*
**Corresponding authors: cristina.grigoras@ub.ro, lgavrila@ub.ro*

the human and animals state of health causing severe skin irritations [2, 3], respiratory problems [4], liver damages or central nervous system injuries [5].

Therefore, many procedures directed to treat dye containing effluents are tested and the interest in developing and adapting other techniques increases continuously.

One of these methods is represented by the adsorption process. Recognized as an efficient, inexpensive and simple to manage procedure [6], the adsorption can be conducted even by using low cost materials such as biomass prepared from flower spikes [7], alginate [8], chitosan [9, 10], clays [11, 12] composites [13-15], adsorbents obtained from vegetal wastes [16, 17] including olive cake [18], date wastes [19], seeds [20], coffee grounds [21] etc.

The adsorption mechanism relies on different interactions (van der Waals forces, hydrogen bonding, polarity, static interactions, dipole-dipole interactions etc.) occurring between the adsorbent and the adsorbate [22] and on the chemical attractions taking place between them [23]. Its efficiency is strongly influenced by a series of factors related to dye (class type, molecular structure etc.), characteristics of the material possessing adsorbing properties (surface area, regenerating capacity etc.) and to the parameters affecting the process (dye solution pH, its initial concentration, temperature, length of the contact time, adsorbent amount - dye solution volume ratio etc.). These aspects have been the subject of many researches [24-27] which revealed that dyes adsorption represent a very attractive alternative to the costlier other techniques of wastewater treatment [28-30] such as those employing for example immobilized enzymes [31], nanofiltration [32], Fenton oxidation [33], photosynthetic bacteria [34] or biogenic nanomaterials [35]. The already conducted investigations show also that the steps to be followed for establishing the appropriate dye adsorption conditions are time-consuming and require multiple experimental tests.

Based on these considerations, in this work, we have used an absorbent material obtained from cherry stones (CS) by physical activation to eliminate Congo Red (CR) (a frequent anionic azo dye in textile, paper, cosmetic, printing industries) from aqueous solutions. The effect of pH, dye initial concentration and contact time was primarily explored. Then, the acquired data were introduced in computer specific software. Mathematical modeling and simulation were tested for predicting the adequate parameters to be utilized in order to obtain the best results in terms of CR removal. Two different approaches: the Response Surface Methodology (RSM) and the Artificial Neural Network (ANN) were applied. Their choice was based on the fact that they have been reported as procuring precise results for dye adsorption modeling. RSM takes into account the interactions of the involved parameters being helpful for designing the experiments. It fits linear or polynomial functions to the collected data [36-38]. ANN is known as a simple and highly reliable artificial intelligence technique which can connect large sets of variables with the purpose of offering trustful nonlinear mathematical equations [39, 40]. Both methodologies return models verified by statistical tests [41, 42].

RESULTS AND DISCUSSION

Congo Red adsorption process onto cherry stones activated carbon

Table 1. Congo Red dye final concentrations after adsorption on cherry stones activated carbon in different working conditions

Initial dye concentration	200 mg/L	400 mg/L	600 mg/L	800 mg/L	1000 mg/L
Time (min)	Final dye concentration (mg/L) at pH 2				
10	11.172	20.007	26.994	39.812	55.184
20	5.858	7.591	16.007	27.044	37.148
30	3.578	5.448	8.333	15.628	18.621
40	2.022	3.612	5.757	7.911	8.788
55	1.075	2.336	3.212	4.911	6.012
60	0.827	1.272	1.896	2.435	3.312
80	0.803	1.146	1.728	2.045	2.873
90	0.791	1.083	1.644	1.850	2.654
100	0.738	1.018	1.526	1.807	2.496
120	0.631	0.888	1.290	1.722	2.181
150	0.588	0.833	1.272	1.678	2.109
180	0.488	0.779	1.178	1.622	1.899
Time (min)	Final dye concentration (mg/L) at pH 4.5				
10	18.177	29.580	43.797	60.602	78.919
20	11.031	19.930	30.755	45.305	57.978
30	8.390	14.616	20.745	31.961	42.375
40	5.503	9.100	13.129	20.372	25.439
55	3.575	4.879	6.873	10.133	13.208
60	1.822	2.112	2.913	4.054	5.251
80	1.436	1.870	2.686	3.519	4.946
90	1.243	1.750	2.572	3.251	4.794
100	1.210	1.677	2.441	3.111	4.684
120	1.144	1.531	2.179	2.832	4.464
150	0.891	1.169	1.705	2.599	3.693
180	0.594	1.052	1.607	1.998	2.500
Time (min)	Final dye concentration (mg/L) at pH 7				
10	29.782	40.271	57.168	71.181	90.788
20	20.181	30.123	40.01	52.571	70.644
30	11.746	18.205	30.25	41.200	54.707
40	7.101	13.137	20.274	29.786	37.331
55	5.588	8.370	10.774	15.333	21.58
60	2.474	3.273	4.662	6.970	7.981
80	2.050	2.676	4.153	5.690	6.823
90	1.838	2.377	3.899	5.050	6.244
100	1.628	2.298	3.819	4.928	6.014
120	1.207	2.141	3.660	4.683	5.555
150	0.599	1.216	2.638	4.282	5.350
180	0.516	1.178	2.452	3.500	4.210

The results of the adsorption process of Congo Red dye on activated carbon prepared from the cherry stones are represented in Table 1. For all the initial concentrations tested in the experiments, more than 90 % of the pollutant was retained after only 10 minutes of contact between the adsorbent material and the dye solutions. After 180 minutes the adsorption efficiency reached over 99 %. Similar observations were reported by other researches which have studied the CR elimination from aqueous effluents by the help of different adsorbing materials made from biowastes [43] or wood sawdust [44]. These researches explain that CR exists in its cationic form at acidic *p*H. The experiments showed that a *p*H between 2 and 7 favors the adsorption. Therefore, it can be concluded that the adsorbent surface is able to retain the pollutant due to the electrostatic attraction caused by its positively charged surface. On the contrary, when the experimental program was conduced at higher *p*H (10 and 12) (data not shown here) a very low CR retention was observed confirming the above hypothesis since at alkaline *p*H CR is in anionic form. In this case, HSO_3^- ion will turn into $–SO^3–Na^+$. As consequence, the CR negative charge density will decrease inducing an electrostatic repulsion between the pollutant and the adsorbent surface with unfavorable repercussions on the adsorption process.

RSM modelling

Models fitting

As stated before, RSM is a powerful tool containing multiple designs. The most frequently employed ones, Central composite and Box-Behnken, present limitations in considering the extent of the investigation ranges and/or the inability of including key experimental extreme points. Moreover, the generated equations present unsatisfactory correlation coefficients (with rather reduced values). Due to these facts and in order to characterize the entire adsorption process, it seemed adequate to create a custom central composite design (CCCD). Therefore, a three-factors with three variation levels CCCD consisting of 135 experimental runs (data not showed but retrieved from Table 1), including replications at the center point, was adopted to optimize the experimental data. The response function (the final CR concentration) was expressed by the linear and polynomial equations (1), (2) and (3).

Linear $$Y = 13.9211 + 9.622351A + 5.094307B - 19.0636C \quad (1)$$

Quadratic $$Y = 5.523482 + 9.157365A + 5.690574B - 19.5703C + 3.011641AB - 12.5546AC - 6.83729BC + 1.826601A^2 - 0.849685B^2 + 18.124092C^2 \quad (2)$$

Cubic $$Y = 5.808814 + 5.542864A + 3.895732B - 15.1419C + 2.908154AB - 12.8594AC - 6.94087BC + 1.73932A^2 - 0.79793B^2 + 17.91289C^2 - 2.79414ABC + 0.298217A^2B - 2.35658A^2C - 1.14011AB^2 + 10.96966AC^2 + 1.397214B^2C + 3.728796BC^2 - 0.54938A^3 - 5.6188C^3 \quad (3)$$

where *Y* represent the final dye concentration and *A*, *B* and *C* are the coded values of the initial dye concentration, *p*H and adsorption time, respectively.

The sequential model sum of squares (Table 2) can be viewed in the reduction of the sum of squares error (SSE). A predictor added to a model explains some of the response variability and thereby reduces the error. A sequential sum of squares quantifies how much variability could be explained (increase in regression sum of squares) or alternatively how much error could be reduced (reduction in the error sum of squares). In this study, the sequential model shows a value of 1648.202 for the sum of squares and therefore it favors the selection of the cubic polynomial equation instead of the quadratic model even though this last one is intensively used when RSM is applied.

Table 2. Sequential model sum of squares

Model	Sum of Squares	Degree of freedom	Mean Square	F-value	p-value Prob > F
Mean vs Total	28883.77	1	28883.77	-	-
Linear vs Mean	30965.47	3	10321.82	90.34611	< 0.0001
2FI* vs Linear	6925.197	3	2308.399	36.74498	< 0.0001
Quadratic vs 2FI	6024.829	3	2008.276	124.4959	< 0.0001
Cubic vs Quadratic	1648.202	9	183.1336	57.69459	< 0.0001
Residual	368.2059	116	3.174189	-	-
Total	74815.68	135	554.1902	-	-

*2FI – two factor interaction

The quality of the models (Table 3) was statistically evaluated firstly based on the coefficient of determination (R^2) and by graphical comparison of the predicted vs. measured values (Figure 2).

Table 3. Models summary statistics

Model	Standard deviation	R^2	Adjusted R^2	Predicted R^2	PRESS*
Linear	10.68867	0.67416	0.666698	0.650026	16074.99
Quadratic	4.016374	0.9561	0.952939	0.946682	2448.981
Cubic	1.781625	0.991984	0.99074	0.988706	518.758

*PRESS – Predicted residual error sum of square

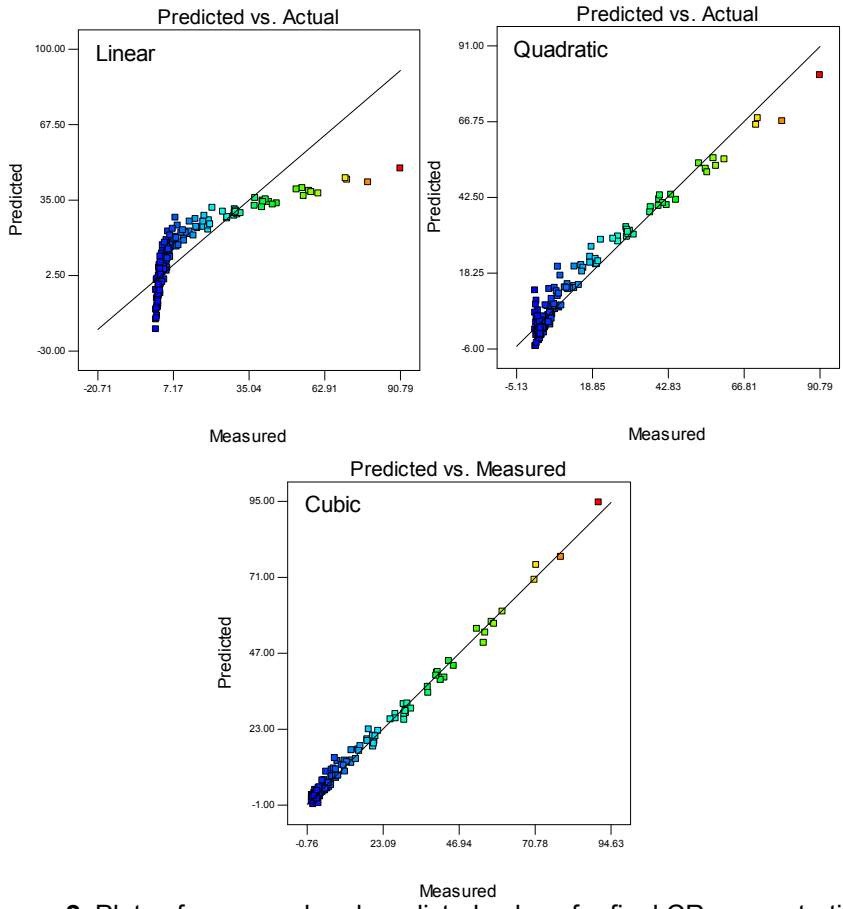

Figure 2. Plots of measured and predicted values for final CR concentration

R^2 is the ratio of the explained variation versus the total variation. It verifies the reliability of an established model. Values of R^2 closer to 1 will better fit the experimental data while a smaller R^2 implies a more reduced similarity between the predicted and the measured records. As noted in Table 3, R^2 is 0.674 for the linear equation, 0.956 for the quadratic model and 0.992 for the cubic one. This means that 32.6 %, 4.4 % and respectively 0.8 % of the total variables for the analyzed response function were not explained by the models. The adjusted R^2 value also explains the accuracy of the model. The important difference between R^2 and adjusted R^2 is that the latter increases only with the addition of input (independent) variables recognized as significant. If non-significant variables are added into the model, the value of adjusted R^2 will decrease, whereas the R^2 will continually

increase. Thus, the smaller gap between R^2 and the adjusted R^2 is desirable for the judgement of a model adequacy. The values of adjusted R^2 of the response show that only 35.0 %, 5.3 % and respectively 1.1 % of the total models variation could not explained.

R^2 values were comparable with those of the predicted R^2 indicating that the models almost perfectly explain the studied experimental range and they can be successfully used to predict the final dye concentration.

Taking into consideration these aspects, it can be concluded that the linear model is the less precise from all and the cubic model has a slight higher degree of confidence then the quadratic one.

The analysis of variance (ANOVA), detailed in Table 4, shows that the generated mathematical equations models were highly significant, because the F-values are greater than 0.001. The *p*-values inferior to 0.0001 means that there are only 0.01 % of the total variation that could not be explained by the model and are attributed to the noise signal.

Table 4. ANOVA results of the RSM models

Source	Sum of Squares	Degree of freedom	Mean Square	F-value	p-value
Linear					
Model	30965.47	3	10321.82	90.34611	< 0.0001
Residual	14966.43	131	114.2476	-	-
Corrected Total	45931.91	134	-	-	-
	Standard deviation	Mean	Coefficient of variance, %	Adequate precision	
	10.68867	14.62716	73.0741	37.64376	
Quadratic					
Model	43915.5	9	4879.5	302.4872	< 0.0001
Residual	2016.408	125	16.13126	-	-
Corrected Total	45931.91	134	-	-	-
	Standard deviation	Mean	Coefficient of variance, %	Adequate precision	
	4.016374	14.62716	27.45833	79.30854	
Cubic					
Model	45563.7	18	2531.317	797.4688	< 0.0001
Residual	368.2059	116	3.174189	-	-
Corrected Total	45931.91	134	-	-	-
	Standard deviation	Mean	Coefficient of variance, %	Adequate precision	
	1.781625	14.62716	12.18025	142.7195	

Adequate precision measures the range in predicted response and its associated error (i.e., a signal-to-noise ratio). Its values were higher than 4 implying desirable fitness of the equations. The coefficient of variance (CV) presents the reproducibility of the models. Expressed as the percent ratio between the standard error of the estimate and the mean value of the observed response, when it is under 10 %, it states that the model can be considered as reasonably reproducible. The cubic and the quadratic models presented the closest values (12.18 % and 27.45 % respectively) to the targeted 10 % of CV while the linear mathematical model has a CV of 73.07 %. Therefore, it was not submitted to more advanced statistical analyses.

Table 5 shows the ANOVA of the quadratic model coefficients for the response indicating that eight terms, namely A, B, C, AB, AC, BC, A^2 and C^2 were found out to be statistically significant ($p < 0.0001$) for the studied response function. The quadratic term A^2, was less significant based on a 95 % confidence level ($p < 0.05$). The lowest importance was attributed to the quadratic term B^2 ($p < 0.2488$).

The sum of squares (SS) of model components was used to calculate the percentage contributions (PC) for each individual term. For the final dye concentration, the time (C) has the highest level of significance with a contribution of 51.29 % as compared to the other components.

Table 5. ANOVA results for the quadratic model coefficients

Factor	Coeffi-cient	95% Confidence interval		Standard error	F-value	p-value	Sum of squares	Contri-bution (%)
		Low	High					
Y, Final pollutant concentration								
Intercept	5.523482	3.860511	7.186453	0.840256	-	-	-	-
A	9.157365	8.188344	10.12639	0.489621	349.8013	< 0.0001	5642.736	12.78
B	5.690574	4.851378	6.529771	0.424024	180.1073	< 0.0001	2905.358	6.58
C	-19.5703	-20.6042	-18.5364	0.522412	1403.36	< 0.0001	22637.97	51.29
AB	3.011641	1.826688	4.196593	0.598726	25.30174	< 0.0001	408.1491	0.92
AC	-12.5546	-14.0149	-11.0943	0.737855	289.5119	< 0.0001	4670.192	10.58
BC	-6.83729	-8.10195	-5.57263	0.639001	114.4892	< 0.0001	1846.856	4.18
A^2	1.826601	0.191211	3.461991	0.82632	4.886419	0.0289	78.82412	0.18
B^2	-0.84968	-2.30095	0.601582	0.733286	1.342661	0.2488	21.65882	0.05
C^2	18.24092	16.35712	20.12471	0.951833	367.2586	< 0.0001	5924.346	13.42

Table 6 points the ANOVA applied for the cubic model coefficients of the response function indicating that sixteen terms A, B, C, AB, AC, BC, A^2, B^2, C^2, ABC, A^2C, AB^2, AC^2, B^2C, BC^2 and C^3 were found out to be statistically significant ($p < 0.0001$) for the adsorption process. The other terms of the model as the quadratic term B^2 and his interaction with initial concentrations and time (A^2B, AB^2, B^2C) and the cubic term A^3 were highly significant based on a 95 % confidence level ($p < 0.05$), meaning that the variable *p*H did not have an intense influence on dye removal in the tested experimental range. For the final dye concentration, the time and his interactions (C) showed the highest level of significance.

Table 6. ANOVA results for the cubic model coefficients

Factor	Coefficient	95% Confidence interval		Standard error	F-value	P-value	Sum of squares	Contri-bution (%)
		Low	High					
Y, Final pollutant concentration								
Intercept	5.808814	0.375201	5.065681	6.551948	-	-	-	-
A	5.542864	0.766931	4.023861	7.061866	52.23436	< 0.0001	165.8017	1.02
B	3.895732	0.371286	3.160353	4.631111	110.0932	< 0.0001	349.4566	2.15
C	-15.1419	0.776783	-16.6804	-13.6034	379.9809	< 0.0001	1206.131	7.41
AB	2.908154	0.266004	2.3813	3.435008	119.5252	< 0.0001	379.3956	2.33
AC	-12.8594	0.327725	-13.5085	-12.2103	1539.635	< 0.0001	4887.093	30.04
BC	-6.94087	0.283819	-7.50301	-6.37873	598.0615	< 0.0001	1898.36	11.67
A^2	1.73932	0.36712	1.012193	2.466447	22.44621	< 0.0001	71.24851	0.44
B^2	-0.79793	0.325787	-1.4432	-0.15267	5.998842	0.0158	19.04146	0.12
C^2	17.91289	0.424883	17.07135	18.75442	1777.43	< 0.0001	5641.899	34.68
ABC	-2.79414	0.400866	-3.58811	-2.00018	48.58463	< 0.0001	154.2168	0.95
A^2B	0.298217	0.448927	-0.59094	1.187374	0.441278	0.5078	1.4007	0.01
A^2C	-2.35658	0.553247	-3.45236	-1.2608	18.14369	< 0.0001	57.59152	0.35
AB^2	-1.14011	0.460014	-2.05122	-0.22899	6.142595	0.0146	19.49776	0.12
AC^2	10.96966	0.597115	9.786999	12.15232	337.4976	< 0.0001	1071.281	6.59
B^2C	1.397214	0.490958	0.424809	2.369619	8.099099	0.0052	25.70807	0.16
BC^2	3.728796	0.517117	2.704581	4.75301	51.99484	< 0.0001	165.0415	1.01
A^3	-0.54938	0.722842	-1.98106	0.882299	0.577642	0.4488	1.833547	0.01
C^3	-5.6188	0.812954	-7.22896	-4.00864	47.76998	< 0.0001	151.631	0.93

Figures 3 and 4 illustrate the influence of two factors while maintaining the other constant at coded value of 0 for the quadratic and the cubic mathematical models. Dye initial concentration has negative effect on the adsorption process. On the contrary, the *p*H showed a positive impact but its influence extent passes from slightly less to highly inferior than that of the adsorption time once that initial dye concentrations increase. The adsorption time is the most important parameter and showed a positive effect on dye removal. The major differences between models are the number of negative values generated on the final dye concentrations, the quadratic model being inferior in the data prediction at low level of initial concentrations and *p*H than the cubic one.

Coefficients used for the cubic mathematical model are given in Table 7.

Table 7. Final equation in terms of actual factors

Final dye concentration =		
Quadratic coefficients	Cubic coefficients	Actual parameters
4.141866292	-1.90961894	-
0.034002923	0.016535466	* Init. dye conc.
5.035463556	4.799626589	* *p*H
-0.733780548	-0.089280881	* Time
0.003011641	0.00953296	* Init. dye conc.* *p*H
-0.00069748	-0.001531938	* Init. dye conc.* Time
-0.060775911	-0.150172977	* pH * Time
1.14163E-05	4.09688E-05	* Init. dye conc.^{2}
-0.135949235	-0.12727603	* *p*H^2
0.009007859	0.00757967	* Time^2
-	-6.2092E-05	* Init. dye conc.* *p*H * Time
-	7.45542E-07	* Init. dye conc.^{2} * *p*H
-	-3.27303E-07	* Init. dye conc.^{2} * Time
-	-0.000456044	* Init. dye conc.* *p*H^2
-	1.35428E-05	* Init. dye conc.* Time^2
-	0.004967872	* *p*H^2 * Time
-	0.000736552	* *p*H * Time^2
-	-8.58406E-09	* Init. dye conc.^{3}
-	-6.16604E-05	* Time^3

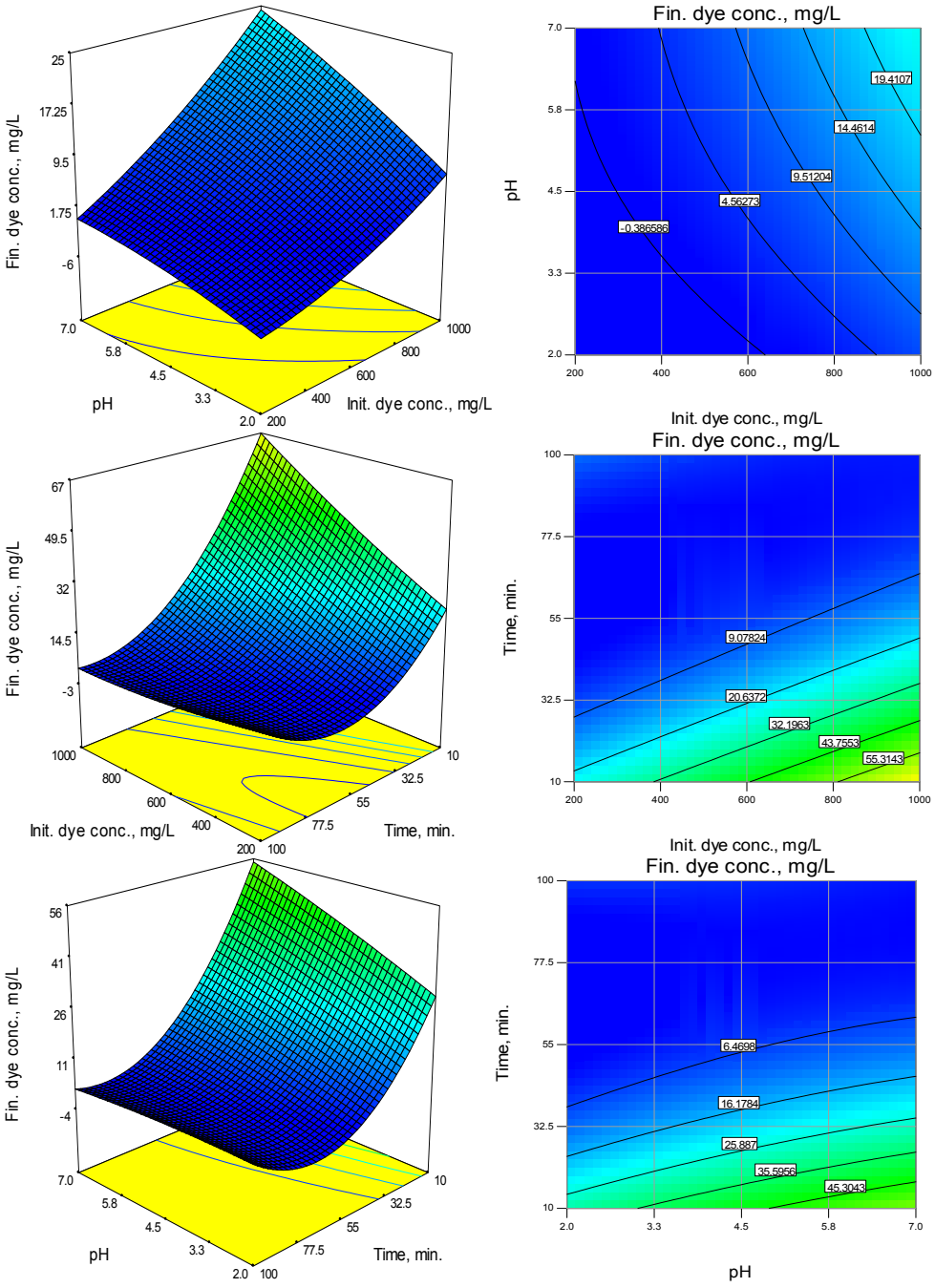

Figure 3. Response surface graphs and contour plots of final dye concentration: the effect of initial dye concentration, *p*H and adsorption time for the quadratic model

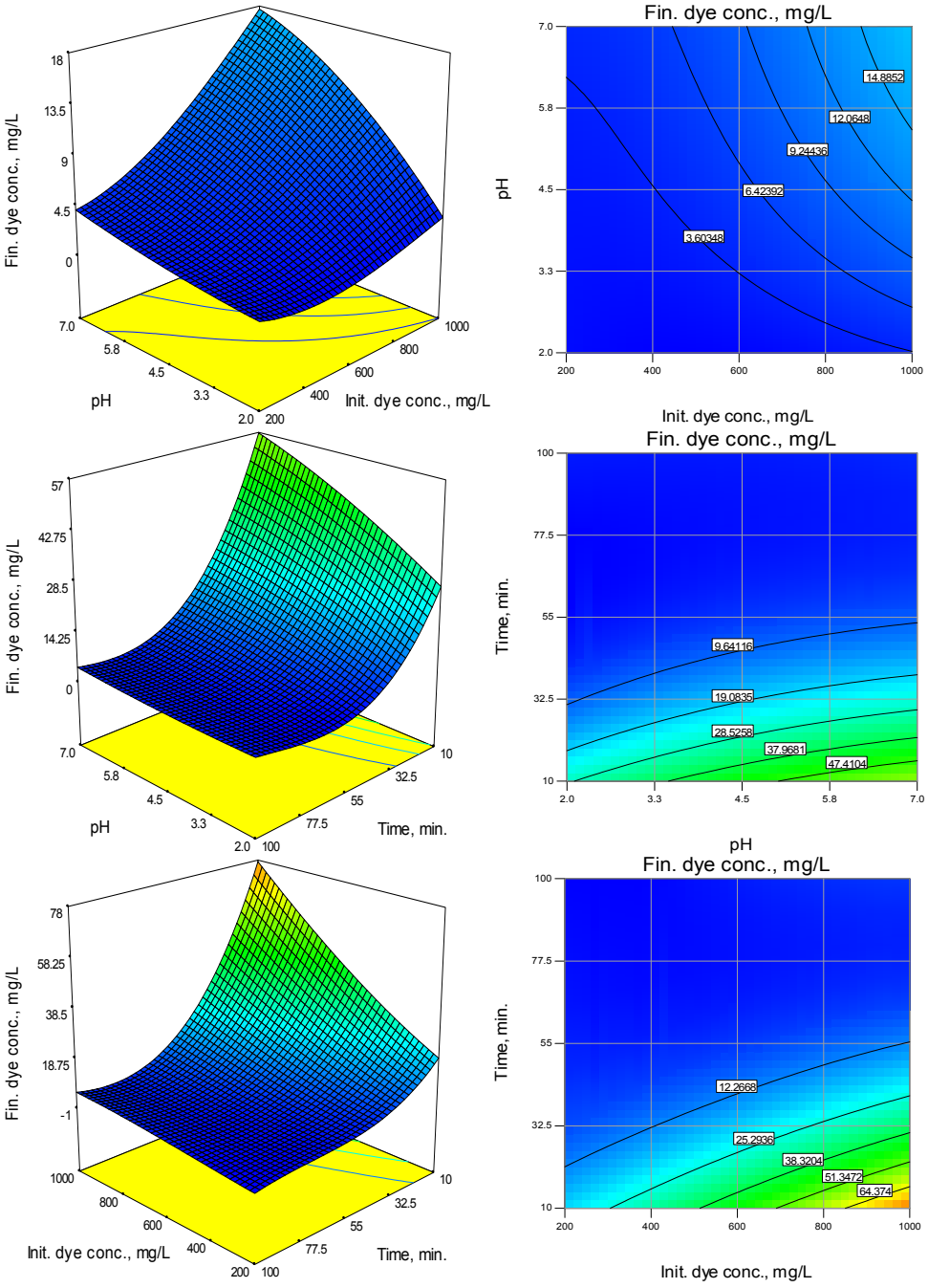

Figure 4. Response surface graphs and contour plots of final dye concentration: effect of initial dye concentration, *p*H and adsorption time for the cubic model

Testing the model

The adopted mathematical model was tested in the conditions planed in the experimental setup A comparison of measured Congo Red final concentrations when dye adsorption from solutions with initial concentrations varying between 200 mg/L and 1000 mg/L was conducted at *p*H 4.5 for 10 to 100 minutes and data predicted by the cubic model is reported in Table 8 as an example. Only minor differences were distinguished. These outcomes along with the similar results registered for runs carried out at *p*H 2.0 and 7.0 (data not shown) sustain also the model adequacy.

Table 8. Measured final dye concentrations at *p*H 4.5 vs predicted by cubic model

Initial dye conc.	**200 mg/L**		**400 mg/L**		**600 mg/L**		**800 mg/L**		**1000 mg/L**	
Time (min)	Final dye concentration, mg/L									
	M	P	M	P	M	P	M	P	M	P
10	18.177	19.756	29.580	30.889	43.797	44.482	60.602	60.124	78.919	77.401
20	11.031	13.007	19.930	20.937	30.755	31.066	45.305	42.980	57.978	56.269
30	8.390	8.238	14.616	13.508	20.745	20.713	31.961	29.443	42.375	39.285
40	5.503	5.081	9.100	8.230	13.129	13.055	20.372	19.141	25.439	26.078
55	3.575	3.164	4.879	4.736	6.873	7.720	10.133	11.705	13.208	16.279
60	1.822	2.117	2.112	2.653	2.913	4.340	4.054	6.765	5.251	9.517
80	1.436	1.157	1.870	1.246	2.686	1.962	3.519	2.893	4.946	3.627
90	1.243	0.503	1.750	1.181	2.572	2.224	3.251	3.221	4.794	3.758
100	1.210	-0.760	1.677	1.049	2.441	2.961	3.111	4.565	4.684	5.448

*M – measured value, P – predicted value

ANN modelling

A selection of data presented in Table 1 was employed for building a feed forward multilayer perceptron's ANN. The values of the three parameters influencing the adsorption procedure (initial dye concentration, *p*H and time) were used as inputs while the final dye concentration was considered as output. The network was trained on 70 % of the input data. The cross validation and the final testing were each managed on 15 % of the inputs. After various trials, a 3 neurons hidden layer with then process elements on the first layer, five process elements on the second and four process elements on the third layer lead to the best results.

At 10000 epochs, the training and the cross validation mean squared errors (MSE) overlay almost perfectly. The MSE insignificant values of 0.000430891 and of 0.000365063 respectively allow to consider that the developed network defines with high confidence the adsorption process evolution.

The analysis of experimental recorded final dye concentrations and of those predicted by ANN (Table 9) discloses as well no significant dissimilarities. Thus, the chosen ANN can offer a correct fact sustained by the high value of the correlation coefficient (0.9926) and by the low value of the minimum square error (13.61).

Table 9. Measured final dye concentrations vs predicted by ANN model

Run	Initial dye concentration, mg/L	*p*H	Time, min.	Final dye concentration, mg/L	
				Measured	Predicted
1	200	2	10	11.172	11.196
2	200	2	20	5.858	6.949
3	200	2	40	2.022	2.785
4	200	2	50	1.075	1.021
5	400	2	30	5.448	6.869
6	400	2	90	1.083	1.147
7	600	2	60	1.896	1.467
8	600	2	80	1.728	1.446
9	800	2	50	4.911	3.771
10	800	2	60	2.435	2.040
11	800	2	80	2.045	1.861
12	800	2	90	1.85	2.183
13	1000	2	20	37.148	36.641
14	1000	2	30	18.621	20.792
15	1000	2	50	6.012	4.550
16	400	4.5	50	4.879	4.548
17	400	4.5	90	1.7495	2.022
18	800	4.5	30	31.961	29.506
19	800	4.5	40	20.372	17.766
20	800	4.5	60	4.054	5.106
21	1000	4.5	10	78.919	69.129
22	1000	4.5	50	13.208	12.197
23	1000	4.5	100	4.684	4.495
24	200	7	30	11.746	12.720
25	400	7	20	30.123	29.439
26	400	7	40	13.137	12.952
27	400	7	50	8.37	7.506
28	600	7	20	40.01	42.683
29	600	7	30	30.25	30.035
30	600	7	40	20.274	19.401
31	600	7	90	3.899	3.613
32	800	7	80	5.69	4.557
33	1000	7	10	90.788	72.717
34	1000	7	90	6.244	5.214

Figure 5 shows the measured values versus the predicted responses indicating that the ANN model almost perfectly explains the studied experimental range and can be successfully used to predict the dye final concentration.

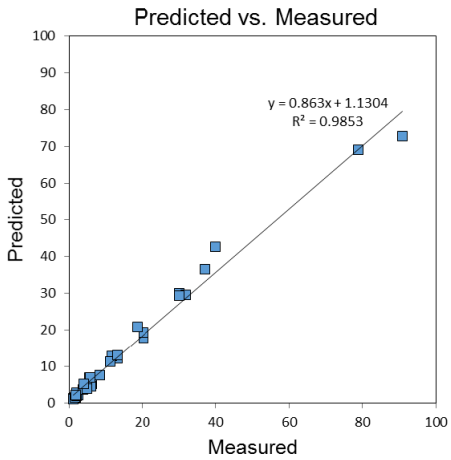

Figure 5. Plot of measured and predicted values for final CR concentration

CONCLUSION

The present research reveals that Congo Red dye is adsorbed on activated carbon obtained by physical activation method from cherry stones, in acidic and neutral media, more than 99 % of the existing dye being removed after 180 minutes.

Even though there were drawbacks in finding the appropriate mathematical models for describing the adsorption of Congo Red dye when influenced by multiples process parameters, this paper emphasizes the successful possibility of using Response Surface Methodology (RSM) and Artificial Neural Network (ANN) for generate adequate equations that fit the recorded experimental data and illustrate their behavior with a high confidence level.

The third-degree polynomial (cubic) model obtained with RSM can be efficiently employed to predict the residual dye concentrations all over the established parameters ranges: initial concentration from 200 mg/L to 1000 mg/L, *p*H from 2 to 7 and contact time between the pollutant and the adsorbent material from 10 minutes to 180 minutes. ANN modelling conducted also to reliable results but contrary to the cubic model, it cannot be emulated in usual computer software's such as Excel spreadsheet requiring only dedicated professional programs which represent a limiting factor for the interested users.

EXPERIMENTAL SECTION

Reagents

Congo Red (CR) dye (Sigma Aldrich, France) solutions with concentrations of 200 mg/L, 400 mg/L, 600 mg/L 800 mg/L and 1000 mg/L were obtained with distilled water.

Sodium hydroxide 0.1 N or hydrochloric acid 0.1 N, procured from Chemical Company (Iasi, Romania), were added in order to insure specific *p*H values of 2, 4.5, 7, 10 and 12.

Adsorbent preparation

Cherry stones used for the adsorbent material preparation were firstly washed then dried at room temperature and crushed.

The resulted powder was calcinated at 600 °C for 4 h in a Caloris L1003 laboratory furnace (Caloris Group, Romania) and the product (abbreviated as CS) was kept at 20 °C in closed vessels until further use.

Adsorption setup

0.1 g of CS were introduced in 50 mL Erlenmeyer flasks. 20.0 mL of CR solution having the anteriorly mentioned concentrations and pH were added.

The adsorption experiments were executed at room temperature on Nahita Blue 692 heating plates (Auxilab, Spain) for 10, 20, 30, 40, 55, 60, 80, 90, 100, 120, 150 and 180 minutes.

The solid phase was eliminated with the help of a Nahita 2615/1 digital centrifuge (Auxilab, Spain) set at 3000 rpm for 5 minutes.

The CR concentration was determined by UV-VIS spectrometry (Zuzi 4201 UV-VIS spectrophotometer, Auxilab, Spain) at specific maximum absorbance wavelengths (570 nm for *p*H 2; 530 nm for *p*H 4.5 and 500 nm for *p*H 7, 10 and 12).

The adsorption efficiency was calculated with the equation (4):

$$Adsorption\ efficiency\ (\%) = \frac{C_0 - C_e}{C_0} \times 100 \quad (4)$$

where C_0 and C_e are the initial and final dye concentration, respectively.

RSM modelling

All data recorded from the experimental program were introduced in two computer software's with the special aim of finding mathematical models able to describe the adsorption process.

Response Surface Methodology (RSM) with custom central composite design (CCCD) based on a three factors and three levels of variation setup was performed using Design-Expert 7.0 software. The regression procedure fitted the polynomial models represented by the equations (5), (6) and (7).

Linear $$Y = \beta_0 + \sum_{i=1}^{k} \beta_i X_i + e_0 \quad (5)$$

Quadratic $$Y = \beta_0 + \sum_{i=1}^{k} \beta_i X_i + \sum_{i=1}^{k} \beta_{ii} X_i^2 + \sum_{i=1}^{k} \sum_{j=i+1}^{k} \beta_{ij} X_i X_j + e_0 \quad (6)$$

Cubic $$Y = \beta_0 + \sum_{i=1}^{k} \beta_i X_i + \sum_{i=1}^{k} \beta_{ii} X_i^2 + \sum_{i=1}^{k} \beta_{iii} X_i^3 + \sum_{i=1}^{k} \sum_{j=i+1}^{k} \beta_{ij} X_i X_j + \sum_{i=1}^{k} \sum_{j=i+1}^{k} \beta_{iij} X_i^2 X_j + + \sum_{i=1}^{k} \sum_{j=i+1}^{k} \beta_{ijj} X_i X_j^2 + \sum_{i=1}^{k} \sum_{j=1+1}^{k} \sum_{j=i+1}^{k} \beta_{ijk} X_i X_j X_k + e_0 \quad (7)$$

Herein, Y is the predicted response (final dye concentration); X_i and X_j are variables; β_0 is the constant coefficient; β_i is the coefficient that determines the influence of parameter i in the response (linear term), β_{ij}, β_{ijk}, β_{iij}, β_{ijj} are the cross-products, coefficient β_{ii} is the quadratic coefficient and β_{iii} is the cubic coefficient, which refer to the effects of the interaction among independent variables. The multiple regression analysis can be applied to obtain the coefficient, and the equation can be used to predict the response.

The coded values (Table 9) of the parameters can be determined from the following equation:

$$x_i = \frac{X_i - X_o}{\delta X} \quad (8)$$

X_0 is the real value of the independent variable at the center point, X_i is the real value of the independent variable, and δX is the step change values between low (−1) and high (+1) levels.

Table 9. Experimental ranges and levels of the independent test variables

Variables	Unit	Symbol	Coded variable level		
			-1	0	1
Initial dye concentration	mg/L	A	400	600	800
*p*H	-	B	2.0	4.5	7.0
Time	min.	C	10	55	100

ANN modelling

Data employed for the Response Surface Methodology design were chosen as inputs and outputs in an Artificial Neural Network three-layered feed forward momentum type. Hidden layers with two to twelve neurons were tried with NeuroSolutions 6.0 software. Three input and one output node with 10000 epochs were used for ANN training.

REFERENCES

1. N. Ribeiro de Mattos; C. Rodrigues de Oliveira; L.G. Brogliato Camargo; R.S. Rocha da Silva; R. Lassarote Lavall; *Sep. Purif. Technol.*, **2019**, *209*, 806-814
2. H. Park; J.-H. Hwang; J.-S. Han; B.-S. Lee; Y.-B. Kim; K.-M. Joo; M.-S. Choi; S.-A. Cho; B.-H. Kim; K.-M. Lim; *Food Chem. Toxicol.*, **2018**, *121*, 360-366
3. C. Goebel; T.L. Diepgen; B. Blomeke; A.A. Gaspari; A. Schnuch; A. Fuchs; K. Schlotmann; M. Krasteva; I. Kimber; *Regul. Toxicol. Pharm.*, **2018**, *95*, 124-132
4. K.B. Tan; M. Vakili; B.A. Horri; P.E. Poh; A.Z. Abdullah; B. Salamatinia; *Sep. Purif. Technol.*, **2015**, *150*, 229-242
5. Y. Gao; S.-Q. Deng; X. Jin; S.-L. Cai; S.-R. Zheng; W.-G. Zhang; *Chem. Eng. J.*, **2019**, *357*, 129-139
6. D. Jiang; M. Chen; H. Wang; G. Zeng; D. Huang; M. Cheng; Y. Liu; W. Xue; Z. Wang; *Coordin. Chem. Rev.*, **2019**, *380*, 471-483
7. Z. Jia; Z. Li; T. Ni; Z. Li; *J. Mol. Liq.*, **2017**, *229*, 285-292
8. A. Oussalah; A. Boukerroui; A. Aichour; B. Djellouli; *Int. J. Biol. Macromol.*, **2019**, *124*, 854-862
9. G.L. Dotto; J.M.N. Santos; E.H. Tanabe; D.A. Bertuol; E.L. Foletto; E.C. Lima; F.A. Pavan; *J. Clean. Prod.*, **2017**, *144*, 120-129
10. H. Ma; A. Kong; Y. Li; B. He; Y. Song; J. Li; *J. Clean. Prod.*, **2019**, *214*, 89-94
11. I. Chaari; E. Fakhfakh; M. Medhioub; F. Jamoussi; *J. Mol. Struct.*, **2019**, *1179*, 672-677
12. W. Hamza; N. Dammak; H.B. Hadjltaief; M. Eloussaief; M. Benzina; *Ecotox. Environ. Safe.*, **2018**, *163*, 365-371
13. M. Tanzifi; M.T. Yaraki; M. Karami; S. Karimi; A.D. Kiadehi; K. Karimipour; S. Wang; *J. Colloid. Interf. Sci.*, **2018**, *519*, 154-173
14. A.M. Herrera-Gonzalez; M. Caldera-Villalobos; A.-A. Pelaez-Cid; *J. Environ. Manage.*, **2019**, *234*, 237-244
15. D.P. Dutta; S. Nath; *J. Mol. Liq.*, **2018**, *269*, 140-151
16. J. Mo; O. Yang; N. Zhang; W. Zhang; Y. Zheng; Z. Zhang; *J. Environ. Manage.*, **2018**, *227*, 395-405
17. K.A. Adegoke; O.S. Bello; *Water Res. Ind.*, **2015**, *12*, 8-24
18. K.H. Toumi; M. Bergaoui; M. Khalfaoui; Y. Benguerba; A. Erto; G.L. Dotto; A. Amrane; S. Nacef; B. Ernst; *J. Mol. Liq.*, **2018**, *271*, 40-50

19. M. Wakkel; B. Khiari; F. Zagrouba; *J. Taiwan. Inst. Chem. E.*, **2019**, *96*, 439-452
20. N.K. Soliman; A.F. Moustafa; A.A. Aoud; K.S.A. Halim; *J. Mater. Res. Technol.*, **2018**, https://doi.org/10.1016/j.jmrt.2018.12.010
21. X. Wen; H. Liu; L. Zhang; J. Zhang; C. Fu; X. Shi; X. Chen; E. Mijowska; M.-J. Chen; D.-Y. Wang; *Bioresource Tehnol.*, **2019**, *272*, 92-98
22. S. Dawwod; T.K. Sen; *J. Chem. Proc. Eng.*, **2014**, *1*, 1-11
23. T. Ngulube; J.R. Gumbo; V. Masindi; A. Maity; *J. Environ. Manage.*, **2017**, *191*, 35-57
24. K. Vikrant; B.S. Giri; N. Raza; K. Roy; K.-H. Kin; B.N. Rai; R.S. Singh; *Bioresource Technol.*, **2018**, *253*, 355-367
25. M.C. Collivignarelli; A. Abba; M.C. Miino; S. Damiani; *J. Environ. Manage.*, **2019**, *236*, 727-745
26. E. Li; B. Mu; Y. Yang; *Bioresource Technol.*, **2019**, *277*, 157-170
27. H.N. Tran; S.-J. You; A. Hosseini-Badegharaei; H.-P. Chao; *Water Res.*, **2017**, *120*, 88-116
28. C.X.-H. Su; L.W. Low; T.T. Teng; Y.S. Wong; *J. Environ. Chem. Eng.*, **2016**, *4*, 3618-3631.
29. M.M. Hassan; C.M. Carr; *Chemosphere*, **2018**, *209*, 201-219
30. C.R. Holkar; A.J. Jadhav; D.V. Pinjari; N.M. Mahamuni; A.B. Pandit; *J. Environ. Manage.*, **2016**, *182*, 351-366
31. L.Y. Jun; L.S. Yon; N.M. Mubarak; C.H. Bing; S. Pan; M.K. Danquah; E.C. Abdullah; M. Khalid; *J. Environ. Chem. Eng.*, **2019**, *7*, 1-14
32. M.A. Abdel-Fatah; *Ain Shams Eng. J.*, **2018**, *9*, 3077-3092
33. M.-H. Zhang; H. Dong; L. Zhao; D.-E. Wang; D. Meng; *Sci. Total Environ.*, **2019**, *670*, 110-121
34. A. Talaiekhozani, S. Rezania; *J. Water Process Eng.*, **2017**, *19*, 312-321
35. P.K. Gautam; A. Singh; K. Misra; A.K. Sahoo; S.K. Samanta; *J. Environ. Manage.*, **2019**, *231*, 734-748
36. S. Karimifard; M.R.A. Moghaddam; *Sci. Total Environ.*, **2018**, *640-641*, 772-797
37. S. Khamparia; D. Jaspal; *J. Environ. Manage.*, **2017**, *201*, 316-326
38. A.K.S. Priya; B.S. Kaith; N. Sharma; J.K. Bhatia; V. Tanwar; S. Panchal; S. Bajaj; *Int. J. of. Biol. Macromol.*, **2019**, *124*, 331-345
39. A.M. Ghaedi; A. Vafaei; *Adv. Colloid Interfac.*, **2017**, *245*, 20-39
40. M.R. Gadekar; M.M. Ahammed; *J. Environ. Manage.*, **2019**, *231*, 241-248
41. A. Simion; C.G. Grigoraş; A. Chiriac; N.C. Tâmpu; L. Gavrilă; *Environ. Eng. Manag. J.*, **2018**, *17*, 771-781
42. A.I. Simion; I. Ioniţă; C.G. Grigoraş; L. Favier-Teodorescu; L. Gavrilă; *Environ. Eng. Manag. J.*, **2015**, *14*, 277-288
43. S. Kaur; S. Rani; K. Mahajan; *J. Chem.*, **2013**, http://dx.doi.org/10.1155/2013/628582
44. C. Tian; C. Feng; M. Wei; Y. Wu; *Chemosphere*, **2018**, *208*, 476-483